

higher transitions was measured for both the $\mu-K$ and $\mu-L$ series and was quite independent of the target material. This is incompatible with an extreme distribution such as (14)¹. Therefore, we conclude that high- l states must be favored, but moderately.

Thus it appears that the observed discrepancy between experiment and the calculated Auger values cannot be simply explained by assumptions about the meson capture distribution and the subsequent cascade process. A more refined examination than that described

in the foregoing produces only greater disagreement. For example, no account was taken of the depletion of the K and L electrons due to previous Auger transitions. Such depletion would clearly reduce Auger competition. Of course, it is possible that the observed decrease at low Z is the result of some mechanism other than Auger competition. We cannot think of any likely prospect. Whatever the mechanism, its Z dependence is similar to that of the Auger effect in view of the good fit of Eq. (1) to the experimental points.

Nonradiative Absorption of Positive Pions by Deuterons at 118 Mev*†

CHARLES ERWIN COHN‡

The Enrico Fermi Institute for Nuclear Studies, The University of Chicago, Chicago, Illinois

(Received November 29, 1956)

The reaction $\pi^+ + d \rightarrow p + p$ was studied at a center-of-mass pion energy of 118 ± 2 Mev, using scintillation counters and a liquid deuterium target. The angular distribution was given by $d\sigma/d\Omega \propto A + \cos^2\theta$, with $A = 0.216 \pm 0.033$, while the total cross section was 12.09 ± 0.93 mb. The total cross section for the inverse pion production reaction was calculated from detailed balancing as 3.10 ± 0.24 mb. These results are compared with other work.

I. INTRODUCTION

THE pion production reaction $p + p \rightarrow \pi^+ + d$ and the inverse nonradiative pion absorption reaction $\pi^+ + d \rightarrow p + p$ have been investigated by many workers, and data are available on total cross sections and angular distributions at center-of-mass pion energies up to 156.5 Mev. Most of the data has been compiled by Rosenfeld¹ with later work reported by Crawford and Stevenson,² Meshcheryakov *et al.*,^{3,4} and Rogers and Lederman.⁵ The work on total cross sections for the higher energies is shown on Fig. 1, while that on angular distribution is plotted on Fig. 2. The data on Fig. 1, both from production and absorption measurements, are plotted in terms of the production cross section; the absorption cross section being related to the former by a simple detailed balancing relationship.⁶

This paper describes measurements of the absorption reaction at a pion c.m. energy of 118 ± 2 Mev. These were

done mainly to test the hypothesis of Meshcheryakov that the angular distribution parameter A is substantially constant between 70 and 160 Mev. However, the results of Stadler⁷ suggest a rise with energy in this region. This question is of special interest because the $(\frac{3}{2}, \frac{3}{2})$ pion-nucleon resonance would be expected to take effect in this region.

The present results are in substantial agreement with Meshcheryakov. The implications are discussed in terms of the phenomenological theory.

II. THEORY

At present, the best interpretation and correlation of these data are given by a phenomenological theory of Gell-Mann and Watson,⁸ who assume that the pion participates in these reactions only in S or P angular momentum states. With this assumption, it is possible to enumerate the quantum states between which the reaction may take place. The result is shown in Table I,

TABLE I. Possible processes for reaction $\pi^+ + d \rightleftharpoons p + p$ with pion in S or P states.

Pion angular momentum state	Total J for pion-deuteron system	$p + p$ state	Cm angular dist. of reaction prod. for isolated case
S	1	3P_1	isotropic
P	0	1S_0	isotropic
P	2	1D_2	$\frac{1}{3} + \cos^2\theta$

* Research supported by a joint program of the Office of Naval Research and the U. S. Atomic Energy Commission.

† Based on a thesis submitted to the Faculty of the Department of Physics, the University of Chicago, in partial fulfillment of the requirements for the Ph.D. degree.

‡ Present address: Argonne National Laboratory, P. O. Box 299, Lemont, Illinois.

¹ A. H. Rosenfeld, Phys. Rev. **96**, 139 (1954).

² F. S. Crawford and M. L. Stevenson, Phys. Rev. **97**, 1305 (1955).

³ M. G. Meshcheryakov *et al.*, Doklady Akad. Nauk S.S.S.R. **100**, 673 (1955).

⁴ M. G. Meshcheryakov *et al.*, Doklady Akad. Nauk S.S.S.R. **100**, 677 (1955).

⁵ K. C. Rogers and L. M. Lederman, Nevis Cyclotron Laboratories Report 25 (unpublished).

⁶ W. B. Cheston, Phys. Rev. **83**, 1118 (1951).

⁷ H. L. Stadler, Phys. Rev. **96**, 496 (1954).

⁸ M. Gell-Mann and K. M. Watson, Annual Review of Nuclear Science (Annual Reviews, Inc., Stanford, 1954), Vol. 4, p. 219.

which gives all the allowable cases. There is one case with total angular momentum $J=1$, a pion S state, and a triplet proton spin state, and two cases with $J=0$ and $J=2$ involving pion P states and singlet proton spin states.

In combining to yield the observed reaction, interference effects may appear between the $J=0$ and $J=2$ cases. However, there may be no interference between these and the $J=1$ case, because of the orthogonality of the singlet and triplet proton spin functions. For the observed reaction, the total cross section will be expressible as

$$\sigma = \alpha\eta + \beta\eta^3, \quad (1)$$

where the first term arises from the pion S state and the second from the pion P states. Here η is the pion c.m. momentum in units of μc .

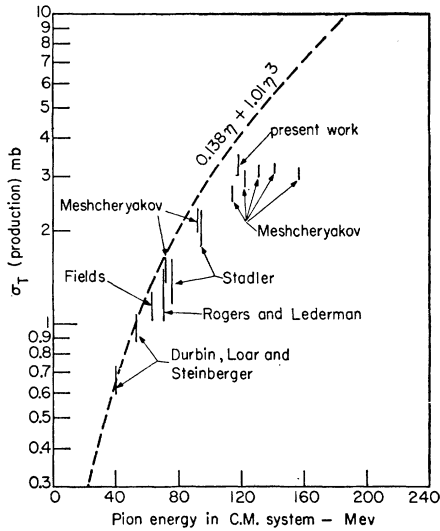


FIG. 1. Total cross section data for reaction $\pi^+ + d \rightarrow p + p$.

The differential cross section will be proportional to $A + \cos^2\theta$, where

$$A = X + (X + \frac{1}{3})\alpha/\beta\eta^2. \quad (2)$$

Here the first term is the isotropic part of the pion P -wave contribution, while the second term is the wholly isotropic S -wave contribution. The parameter X is a function of the interference between the two pion P -wave cases, and can be expressed as a function of the ratio δ_0 between the reaction amplitudes of the $J=0$ and $J=2$ cases:

$$1/X = \left| \frac{2 - \sqrt{2}\delta_0}{1 + \sqrt{2}\delta_0} \right|^2 - 1. \quad (3)$$

The parameters α , β , and X have been determined empirically by Crawford and Stevenson.²

Substitution of these into Eqs. (1) and (2) yields the expressions

$$\begin{aligned} \sigma &= 0.138\eta + 1.01\eta^3, \\ A &= 0.082 + 0.057\eta^{-2}, \end{aligned} \quad (4)$$

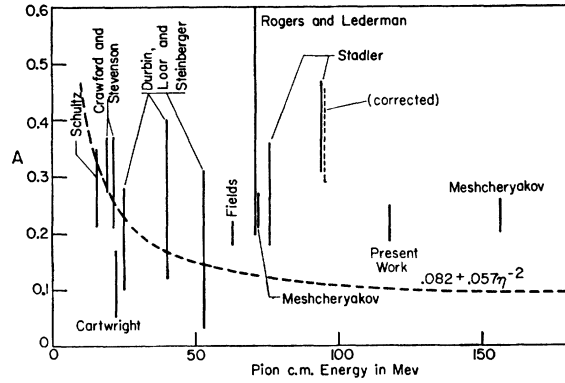


FIG. 2. Angular distribution data for reaction $\pi^+ + d \rightarrow p + p$. $d\sigma/d\Omega \propto A + \cos^2\theta$.

for total cross section and angular distribution. These functions are plotted on Figs. 1 and 2. They make a good fit to the experimental data below about 50 Mev, but show marked deviations at the higher energies.

The deviations from Eq. (4) for total cross section are most marked for the data of Meshcheryakov,⁴ which lie considerably below the curve and suggest a possible resonance around 140 Mev. These deviations need not cause excessive concern, because the assumptions underlying Eq. (1) cannot be expected to hold far above threshold, especially if there is a resonance.

In deriving Eq. (5), the theory assumes that δ_0 and hence X are constant with energy. However, this assumption would break down if the $(\frac{3}{2}, \frac{3}{2})$ resonance were operative, since this resonance would enhance only the $J=2$ state. Thus δ_0 and X could be expected to vary over the region of resonance, and Eq. (5) would not be expected to hold. Most of the experimental data, however, with the exception of Stadler, indicates that above 70 Mev the value of A becomes constant, but at a higher level than predicted by Eq. (5).

III. EXPERIMENTAL METHOD

The reaction was studied by irradiating a liquid deuterium target with a positive pion beam from the Chicago synchrocyclotron. The target is essentially as described by Stadler, with some subsequent changes to improve the efficiency of liquefaction. The pion beam was brought out of the cyclotron using the apparatus and techniques described by Warshaw and Wright.⁹ The geometry used is shown in Fig. 3 with the counters used listed in Table II. The incident beam passes through counters 1 and 2 on its way to the target, coincidences between these counters being used to define incident pions.

The general features of the geometry are dictated by the necessity to observe the absorption reaction with full efficiency while rejecting counts due to other

⁹ S. D. Warshaw and S. C. Wright, Rev. Sci. Instr. (to be published).

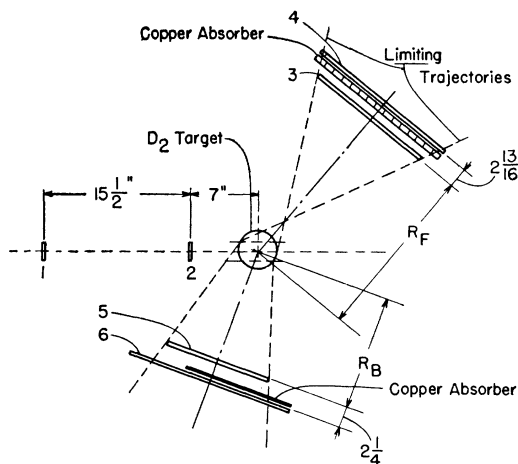


FIG. 3. Geometry for absorption measurements.

possible pion-deuteron reactions. This problem has been considered by Stadler, and the type of setup which he used was adopted as a starting point. This consisted of a counter placed on each side of the target to record both protons, together with absorbers placed in front of the counters to stop recoil protons and deuterons from the pion-deuteron scattering reactions.

This simple arrangement does discriminate against the undesired reactions. However, there is a source of spurious counts from the pion-deuteron inelastic scattering, $\pi^+ + d \rightarrow \pi^+ + n + p$. The pions from this reaction can penetrate the counters and be recorded. Although the protons will be stopped by the absorbers, the neutrons can penetrate the absorbers and make countable recoils in the counters. This can produce an effect about 3% of the desired one. It can be eliminated, though, by placing another counter in front of each absorber. The energy spectrum of the neutrons is such that they cannot make recoils which could penetrate the absorber and record in both counters. Thus the neutrons could only record by making separate recoils in each counter, which reduces the contribution of this reaction to about 1 in 10^4 .

The two remaining possibilities for spurious counts are small and come from the pion-deuteron charge-exchange scattering and radiative absorption, $\pi^+ + d \rightarrow \pi^0 + p + p$ and $\pi^+ + d \rightarrow \gamma + p + p$. The former may contribute if the gamma rays from the decay of the neutral pion each create a pair which is recorded by the

TABLE II. Specifications of counters.

Counter number	Width	Height	Thickness	Material
1	2 in.	2 in.	$\frac{1}{8}$ in.	Plastic
2	2 in.	2 in.	$\frac{3}{32}$ in.	Plastic
3	14 in.	9 in.	5/8 in.	{ 3/8 in. liquid, 1/8 in. walls
4	17 in.	12 in.		
5	11 1/2 in.	7 in.		
6	18 1/4 in.	9 in.		

counters, while the latter may contribute if the energy partition between gamma ray and protons is such that the two protons have the proper energies and angular correlation to be counted. The former reaction contributes about 0.2% and the latter about 0.1%.

In the complete geometry, as shown in Fig. 3, the solid angle is determined by counter 3, since it is farther from the target than counter 5. The counters are so placed and proportioned that every proton entering counter 3 would be accompanied by a correlated proton recording in counter 5. This is shown by the "limiting trajectories" on Fig. 3. The limitation on usable counter widths was the need for a minimum angle small enough to give a sensible angular distribution, while the counter heights were limited by the requirement that all protons counted should pass through the thin-walled sections of the target.

Copper absorbers were placed between the counters as close as possible to the rear counters to reduce scattering losses. They were designed to meet the twin requirements of passing the least energetic protons from the desired absorption reaction, while stopping the most penetrating recoils from the pion-deuteron scattering reactions. These latter were taken to be the protons produced in the charge-exchange scattering with the neutral pion assumed to have zero kinetic energy in the c.m. system. (This reaction gives more energetic protons than the corresponding non-charge-exchange inelastic scattering because the mass difference between charged and neutral pions goes into proton kinetic energy.) The calculations were done taking into account energy loss in the target and in the front counter, as well as the obliquity of some proton trajectories. It was found that the absorbers had to vary in thickness over the width of the counter, being thickest at smaller angles.

Since the differential cross section was believed to depend on two parameters, it was decided to take measurements at three angles. Data concerning the counter radii and angles finally chosen are given in Table III.

For each of the three cases, calculations were made of the product of solid angle and counting efficiency and of the effective c.m. angle which the counters see. (The angle θ_{eff} is the angle whose square cosine equals the average of $\cos^2\theta$ over all possible proton trajectories from the target to counter 3, when allowance is made for the variation of counting efficiency for the various trajectories.) The results of the calculations are given in Table IV.

In the calculation, the area of counter 3 was divided horizontally into seven segments each two inches wide. For each segment, graphical measurements were made of the angular width of the segment, the angle of the ray to the center of the segment and the distance to the center of the segment. All measurements were made in the median plane looking from the center of the target. With $2H$ equal to the counter height in inches, R the

distance in inches, and $d\theta$ the angular width of the segment in the c.m. system, the solid angle for that segment is given by $d\Omega = 0.017543(d\theta)(2H/R)$ in steradians. The quantity $d\Omega$ was summed over all segments to get the total solid angle Ω , which is the first entry in Table IV.

The calculation of counting losses caused by absorption of the protons by the various materials in their path was similar to the method of Stadler.⁷ However, refinements were introduced by using the experimental values of elastic/total cross section ratios instead of the theoretical value of one-half; and by taking into account the increase in path length caused by the obliquity of some proton trajectories in the counters. The cross section data used were those of Millburn *et al.*,¹⁰ De Juren,¹¹ and De Juren and Knable.¹² For each segment, an efficiency e was determined, which is the probability that neither of the two correlated protons be absorbed before registering in all counters. The uncertainty in the absorption due to uncertainty in the cross section data was taken as 10%. Since the absorption was about 20%, the resulting error in the final results was $\pm 2\%$. For each segment, the quantity $e d\Omega$ was calculated, the sum giving the value of $\bar{e}\Omega$ which is given in Table IV.

Also calculated for each segment was the quantity $e d\Omega \cos^2\theta$, where θ was the c.m. angle of the center ray to each segment. This was summed to give $\bar{e}\Omega \cos^2\theta_{\text{eff}}$ which is also entered in Table IV. From these calculated quantities, the numbers \bar{e} and $\cos^2\theta_{\text{eff}}$ can be derived, and are given in the table.

Because of the approximations made in the calculations, it was necessary to make certain small adjustments to the results. First, the adjustment to Ω due to the extended source produced by the finite width of the target ranged from 0.2% to 0.3%. Another adjustment to Ω resulted from the use of H in the expression for $d\Omega$ instead of the correct expression $R \arctan(H/R)$. This ranged from 1.5% to 2.1%.

There were three adjustments made to $\cos^2\theta_{\text{eff}}$. The first was necessitated by the finite height of the counters, since a point on the counter off the median plane is at a different θ than its projection on the median plane. This adjustment ranged from 1.0% to 2.4%. Another adjustment was occasioned by the finite size of the segments and ranged from 0.01% to 1.2%. The third adjustment was necessitated by the finite width of the target and ranged from 0.02% to 1.16%.

The electronic arrangement used in the measurements was essentially as described by Glicksman, Anderson, and Martin¹³ with later modifications as described by Davidon and Frank.¹⁴

¹⁰ G. P. Millburn *et al.*, Phys. Rev. **95**, 1268 (1954).

¹¹ J. De Juren, Phys. Rev. **80**, 27 (1950).

¹² J. De Juren and N. Knable, Phys. Rev. **77**, 606 (1950).

¹³ Glicksman, Anderson, and Martin, Proceedings of the National Electronics Conference, 1953 (unpublished), Vol. 9, p. 483.

¹⁴ W. C. Davidon and R. B. Frank, Rev. Sci. Instr. **27**, 15 (1956).

TABLE III. Proton counter settings.

Case	1	2	3
Angle of counter 3	36°	51°	80°
Radius of counter 3 ^a (R_F)	23 in.	18½ in.	17½ in.
Angle of counter 5	125°	110°	77°
Radius of counter 5 ^a (R_B)	6½ in.	6⅙ in.	6½ in.

^a To front surface of counter sensitive volume.

The energy of the pion beam was determined by taking a range curve. The curve indicated a mean pion range of 67.5 g/cm² of copper, and showed a (7±1)% muon component. No protons, positrons, or other contamination were observed.

Corrections for the thickness of the last counter, and the obliquity of the pion paths in the copper due to multiple scattering¹⁵ make the mean range 69.2 g/cm², corresponding to a pion energy of 146.5 Mev.¹⁶ Since the pions lose 2.5 Mev in traversing one-half of the target, the pion energy at the center of the target came to 144 Mev, corresponding to a c.m. energy of 118±2 Mev. This spread includes uncertainties in the measurements and the energy spread due to the finite target size.

The final quantity of importance is the number of deuterium atoms per cm² in the target which were exposed to the beam. This was obtained with the method described by Nagle¹⁷ using the thermodynamic data of Woolley *et al.*¹⁸ The result was corrected for a 1.51% hydrogen atom contamination as measured by a mass spectrographic analysis¹⁹; and for the cylindrical shape of the target and the finite width of the beam, by taking a beam profile as described by Nagle. The result was 4.778×10^{23} atoms/cm², with a probable error of $\pm 1\%$.

IV. RESULTS

During the cyclotron run, measurements were made at all three angles with deuterium in and out of the

TABLE IV. Solid angle, efficiency, and effective angle calculations.

Case	1	2	3
Calculated quantities:			
Ω	0.26379	0.38916	0.40776
$\bar{e}\Omega$	0.22403	0.33106	0.34285
$\bar{e}\Omega \cos^2\theta_{\text{eff}}$	0.11714	0.08607	0.01693
Derived quantities:			
\bar{e}	0.8493	0.8507	0.8408
$\cos^2\theta_{\text{eff}}$	0.52288	0.25998	0.04938
Adjusted quantities:			
$\bar{e}\Omega$	0.22037	0.32372	0.33479
$\cos^2\theta_{\text{eff}}$	0.5174	0.2596	0.0521
$\bar{\theta}$	44.1°	59.4°	76.8°

¹⁵ W. C. Davidon (private communication).

¹⁶ M. Rich and R. Madey, University of California Radiation Laboratory Report UCRL-2301 (unpublished).

¹⁷ D. E. Nagle, Phys. Rev. **97**, 480 (1955).

¹⁸ Woolley, Scott, and Brickwedde, J. Research Natl. Bur. Standards **41**, 379 (1948).

¹⁹ The author wishes to thank Dr. Dwight Hutchison of Argonne National Laboratory for performing this analysis.

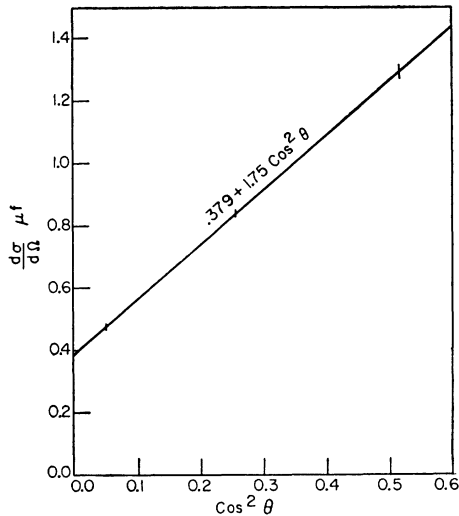


FIG. 4. Observed angular distribution at 118 Mev with fitted line.

target cell. For each measurement, counts were taken of coincidences between counters 1 and 2 ($D12$) and of coincidences between all six counters ($S123456$). Averages of these counts and their standard deviations are given in Table V. About 36×10^6 $D12$ counts with deuterium in and about half that number with deuterium out were taken for each angle. The $D12$ counting rate was about 40 000 per minute.

The counting system was tested for efficiency by placing all counters in the beam with counter 1 in front of and counter 2 behind the others (3456). Doubles 12 ($D12$) and sextuples 123456 ($S123456$) were recorded. Ideally, in this geometry the ratio S/D should be 100%. At the beam intensities used in the measurements, though, the ratio was considerably lower, ranging from 56% to 66% at various times during the run. Although the origin of these losses was not established, their irrelevance in the present experiment was demonstrated by the following tests. The beam intensity was reduced, and it was found that at very low $D12$ rates the ratio approached unity, reaching 96% at about 100/min. In addition, counter 5 was replaced by a small ($\frac{3}{16} \times \frac{5}{16}$) counter normally used for taking beam profiles. Because of its dimensions, this counter recorded only a very small fraction of the flux. Counts were made of sextuple coincidences between this counter (5') and counters 1, 2, 3, 4, and 6. The sextuples to doubles ratio $S12345'6/D12$ was found to be constant within statistical error at beam rates from 83 000/min down to 8100/min. Thus, since the beam rate in the actual experiment was about 40 000/min, it was concluded that the protons from the absorption reaction were counted with 100% efficiency.

Checks were also made to determine the contribution of accidental coincidences to the observed counts. For the sextuples this was done in two ways. First, a delay greater than the resolving time of the coincidence

TABLE V. Results.

Case	1	2	3
$S123456$ per 10^6 $D12$:			
Deuterium in:	281.2 ± 4.2	255.6 ± 3.9	149.7 ± 2.9
Deuterium out:	36.3 ± 2.3	22.5 ± 1.6	13.3 ± 1.2
Net:	244.9 ± 4.8	233.1 ± 4.2	136.4 ± 3.1
$d\sigma/d\Omega$, mb/sterad	1.285 ± 0.027	0.832 ± 0.015	0.470 ± 0.011

circuit was introduced into one of the inputs. When counter 6 was delayed, one $S123456$ count was observed for 500 000 $D12$ counts, and when counter 3 was delayed, no sextuples were observed for the same number of doubles. These counts were done with deuterium in the cell and with the counters set in the geometry of Case 1.

Another check was made by placing counters 3 and 4 so that no proton penetrating them could give rise to a correlated proton in counters 5 and 6. In this arrangement, three sextuples were observed for 500 000 doubles; this was the case both with and without deuterium. Hence it was concluded that the contribution of accidentals to the sextuples counts was negligible. These sextuple accidentals tests were made at the beam intensity used in the experiment proper.

A check on the contribution of accidentals to the doubles count was made, again by delaying one counter sufficiently. The counts so recorded were about 4.5% of the doubles rate. However, not all of these counts are to be interpreted as accidentals. Mesons in the beam, which can give only true doubles coincidences, contributed $\frac{1}{3}$ of the observed singles rates. The true accidentals formed therefore $4.5 \times (2/3)^2 = 2\%$ of the observed doubles rate.

This test was made at 65% of the normal beam intensity (because of reduced cyclotron output) so that the proper correction for accidentals should be $0.02 \times (1/0.65) = 3.1\%$.

Differential cross sections calculated from these counts are also given in Table V. These cross sections were analyzed by the least-squares method to yield the angular distribution. The function used was $d\sigma/d\Omega = a + b \cos^2\theta$, which yielded $a = 0.379 \pm 0.049$ and $b = 1.75 \pm 0.15$. Thus the angular distribution parameter A was 0.216 ± 0.033 , while integration gave the total cross section as 12.09 ± 0.93 mb. Using this number in a detailed-balancing calculation gave the cross section for pion production at the same c.m. pion energy as 3.10 ± 0.24 mb.

All of the above numbers except the total cross sections have been quoted with statistical errors only, since other errors affect all angles equally and thus do not affect the angular distribution. However, all have been corrected for the muon contamination in the beam, for spurious reactions, and for accidentals. The error on the total cross sections includes the uncertainties in the proton absorption cross sections, the deuterium density, and the muon contamination.

The differential cross sections from Table V have

been plotted against $\cos^2\theta$ on Fig. 4, along with the least squares line. The least squares sum is 0.0274 and the corresponding chi-square probability is about 88%, indicating a reasonable fit.

V. DISCUSSION

The relationship between the present work and previous work on these reactions can be seen on Figs. 1 and 2. It is apparent from Fig. 1 that the present value of total cross section is in good agreement with the behavior in this energy region as seen by Meshcheryakov.

Figure 2 appears to support the hypothesis of Meshcheryakov of the constancy of A from 70 to 160 Mev. The 94-Mev point of Stadler has been slightly raised to account for the finite width of his counters and target.²⁰

Now it is necessary to look at the implications of this in terms of the phenomenological theory. We note the

²⁰ H. L. Stadler (private communication).

existence of an apparent resonant behavior as suggested by the total cross-section data. If we attribute that to the $(\frac{3}{2}, \frac{3}{2})$ resonance, the $J=2$ state and not the $J=0$ state would be enhanced. This, as previously explained, implies a variation of δ_0 in the region of resonance, resulting in a variation in X and thus in A . However, this is not observed. Thus it appears that some modification or elaboration of the simple phenomenological theory is needed to deal with the situation in this energy region.

ACKNOWLEDGMENTS

The author wishes to thank Professor Darragh E. Nagle for suggesting the problem and for many helpful discussions during its progress. Thanks are also due to Dr. Willard Skolnik for assistance in taking data, Professor Herbert L. Anderson for the use of his counting equipment, and Professor Earl Long and Professor Lothar Meyer for supplying liquid hydrogen and for valuable assistance in the operation of the deuterium target.

Nuclear Size from Cosmic-Ray Interactions

M. S. SINHA AND N. C. DAS

Bose Institute, Calcutta, India

(Received November 19, 1956)

The total path length of 3625 penetrating charged secondaries of average energy 4 Bev has been measured in three plate assemblies of Al, Cu, and Pb inside a big square cloud chamber. The total number of nuclear interactions observed were divided into two groups, (i) nuclear disintegrations (high-energy transfers) and (ii) nuclear scatterings (elastic), and the *total* cross section and the cross section for nuclear disintegrations alone have been determined. It has been found that the equivalent square-well radii of Al, Cu, and Pb found from the latter cross sections agree well with $1.19A^{1/3} \times 10^{-13}$ cm whereas the radii corresponding to the total cross sections follow $1.34A^{1/3} \times 10^{-13}$ cm. The results thus indicate the same matter distribution in Al, Cu, and Pb nuclei as that determined from high-energy electron scattering, mu-mesonic x-ray data, and high-energy neutron absorption data. Moreover, each nucleus appears to be surrounded by an equivalent spherical shell of thickness $0.15A^{1/3} \times 10^{-13}$ cm which chiefly accounts for the elastic nuclear scatterings. The existence of this shell is presumably the effect of the finite range of nuclear forces.

INTRODUCTION

THE size of the nucleus of various elements has been determined in the past few years from (i) fast electron scattering,¹ (ii) mu-mesonic x-rays,² (iii) high-energy (1.4 Bev) neutron absorption,³ and (iv) ultra-high-energy cosmic-ray data.⁴ While the first two methods give the spatial extension of the nuclear charge, the third one determines the spatial distribution of nuclear matter. The fourth method surprisingly gives values of the size of the nucleus about twenty percent

higher than the first three methods. Williams⁵ has made a critical analysis of all these data and has shown that experimental observations by the first three methods can be reconciled with each other if it is assumed that the nuclear density drops off smoothly at the edge of the nucleus. Furthermore, the larger values of the cross section from cosmic-ray experiments can only be understood on the basis of a nonuniform distribution of density inside the nucleus and a progressive increase of the elementary np and pp scattering cross sections at higher energies (~ 30 Bev). Whereas Williams' analysis is based on the assumption that nuclear matter and charge have the same spatial extension, Johnson and Teller⁶ and Drell⁷ have put forward the

¹ Hofstadter, Fechter, and McIntyre, Phys. Rev. **92**, 978 (1953); D. G. Ravenhall and D. R. Yennie, Phys. Rev. **96**, 239 (1954).

² V. L. Fitch and J. Rainwater, Phys. Rev. **92**, 789 (1953).

³ Coor, Hill, Hornyak, Smith, and Snow, Phys. Rev. **96**, 1369 (1955).

⁴ R. W. Williams, Phys. Rev. **98**, 1393 (1955).

⁵ R. W. Williams, Phys. Rev. **98**, 1387 (1955).

⁶ M. H. Johnson and E. Teller, Phys. Rev. **93**, 357 (1954).

⁷ S. D. Drell, Phys. Rev. **100**, 97 (1955).